

BGK Electron Solitary Waves Reexamined

Li-Jen Chen and George K. Parks*

Physics Department, University of Washington, Seattle, WA 98195

**Also at Space Science Laboratory, University of California, Berkeley*

This paper reexamines the physical roles of trapped and passing electrons in electron Bernstein-Greene-Kruskal (BGK) solitary waves, also called the BGK phase space electron holes (EH). It is shown that the charge density variation in the vicinity of the solitary potential is a net balance of the negative charge from trapped electrons and positive charge due to the decrease of the passing electron density. A BGK EH consists of electron density enhancements as well as a density depletion, instead of only the density depletion as previously thought. The shielding of the positive core is not a thermal screening by the ambient plasma, but achieved by trapped electrons oscillating inside the potential energy trough. The total charge of a BGK EH is therefore zero. Two separated EHs do not interact and the concept of negative mass is not needed. These features are independent of the strength of the nonlinearity. BGK EHs do not require thermal screening, and their size is thus not restricted to be greater than the Debye length λ_D . Our analysis predicts that BGK EHs smaller than λ_D can exist. A width(δ)-amplitude(ψ) relation of an inequality form is obtained for BGK EHs in general. For empty-centered EHs with potential amplitude $\gg 1$, we show that the width-amplitude relation of the form $\delta \propto \sqrt{\psi}$ is common to bell-shaped potentials. For $\psi \ll 1$, the width approaches zero faster than $\sqrt{\psi}$.

PACS numbers: 52.35.Sb, 52.35.Mw, 52.35.Fp

In 1957, Bernstein, Greene and Kruskal [1] solved the one-dimensional, time-independent Vlasov-Poisson equations and obtained the general solutions for electrostatic nonlinear traveling waves, including solitary potential pulses. Their derivation emphasized the special role played by the particles trapped in the potential energy troughs. They demonstrated mathematically that one could construct waves of arbitrary shapes by assigning the distribution of trapped particles suitable for the desired wave form.

In 1967, Roberts and Berk [2] provided a quasi-particle picture for the electron phase space holes (EH) based on the results of a numerical experiment on two-stream instability. They solved the time-dependent Vlasov-Poisson equations using the “water-bag” model in which the evolution of electron phase-space boundaries between $f = 0$ and $f = 1$ was followed, where f is the electron phase space density with values either 0 or 1. They interpreted the elliptical empty ($f = 0$) region associated with a positive charge observed in the late stage of the nonlinear development as a BGK EH. In order to explain the coalescence of neighboring EHs, a negative effective mass was assigned to each EH to compensate for the Coulomb repulsion of two positive EHs. Thus, they suggested a quasi-particle picture that BGK EHs have positive charge and negative mass. This picture is in use even today to interpret results in computer simulations of EH disruptions due to ion motion [3], and to model the mutual interaction of electrostatic solitary waves in space plasma [4].

It was not until 1979 that BGK EHs were experimentally realized by the Risø laboratory experiments [5,6]. By applying large amplitude potential pulses in a plasma-

loaded wave guide, solitary potential pulses were excited, including EHs and Korteweg-de Vries (KdV) solitons [7]. Investigations of the mutual interaction of EHs showed that two EHs close to each other would coalesce if they have almost equal velocity and they would pass through each other if their relative velocity was large [5]. The coalescence was interpreted in terms of the positive EH picture derived earlier [5,6].

The analytical work that followed the Risø experiments mainly focused on constructing solutions and obtaining the corresponding width-amplitude relations to facilitate the comparison between BGK EHs and KdV solitons [8–10]. In addressing the quasi-particle picture of EHs, Schamel [9] concluded that EHs were positively charged, screened by the ambient electrons over many Debye lengths (λ_D), and had negative mass [9]. This conclusion supports the positive EH picture previously obtained from the numerical experiments [2,11] and that the minimum size of EHs of several λ_D is a consequence of thermal screening by the ambient electrons.

Turikov [8] followed the BGK approach and constructed the trapped electron distribution for a Maxwellian ambient electron distribution and for several kinds of solitary potential profiles. He restricted his study to BGK EHs with phase space density zero in a hole center and the results showed that the potential width increases with increasing amplitude. This behavior is different from that of the KdV solitons whose width decreases with increasing amplitude. He also numerically simulated the temporal evolution of the EHs for different Mach numbers to study the EH stability and found that EHs are quasi-stable for Mach numbers less than 2. One of the main conclusions that Turikov made was that EHs

are purely kinetic nonlinear objects in which trapped particles play an important role, but exactly what physical role trapped particles played was not addressed.

Space-borne experiments now show that electrostatic solitary waves (ESW) are ubiquitous in Earth's magnetospheric boundaries, shock, geomagnetic tail and auroral ionosphere [12–19]. While detailed properties of these solitary waves are continuously being studied, it has been shown that in a number of cases the ESWs have features that are consistent with BGK electron [20] and ion [21] mode solitary waves. A statistical study by FAST satellite observations [16,17] in the auroral ionosphere has revealed that solitary pulses with a positive potential typically have a Gaussian half width ranging from less than one λ_D to several λ_D with a mean of $1.80\lambda_D$ and a standard deviation of $1.13\lambda_D$. However, the statistical analysis strongly favored large amplitude pulses [16,17] and smaller EHs if they existed were not sampled. This question of how small EHs can be is an important issue associated with how a collisionless plasma supports nonlinear waves and needs to be further investigated.

To examine the physical roles played by trapped and passing electrons, we start first with simple physical arguments and then perform analytical calculations using the same formulation used by Turikov [8], except we relax the restriction of empty-centered EHs and obtain a more general width-amplitude relation. The number density profiles of trapped and passing electrons are calculated to show that the negative charge density at the flank of the EH comes exclusively from trapped electrons. It is argued that the BGK EH as a physical entity consists of a density enhanced region and a depletion region, and the total charge of the EH is zero. The screening of the positive core is achieved by trapped electrons oscillating between their turning points, and not the thermal screening by the ambient electrons as previously thought. There does not exist a minimum size for BGK EHs based on Debye shielding. In addition, two separated EHs do not interact and the concept of negative mass is not needed. These features are shown to be independent of the strength of the nonlinearity defined by the amplitude of the potential.

We first discuss heuristically the behavior of electrons in the vicinity of a potential pulse. Figures 1(a)-1(c) show the general form of a positive solitary potential pulse ($\phi(x)$), the corresponding bipolar electric field ($E = -\partial\phi/\partial x$) and the total charge density ($\rho = -\partial^2\phi/\partial x^2$). The charge density is positive at the core, negative at the boundary, and zero outside the solitary potential. Figure 1(d) shows the potential energy trough with an electron passing by (open circle) and a trapped electron (solid circle) at its turning point. Consider the phase space trajectories of electrons passing by the potential and those that are trapped in the potential shown in Figure 1(e).

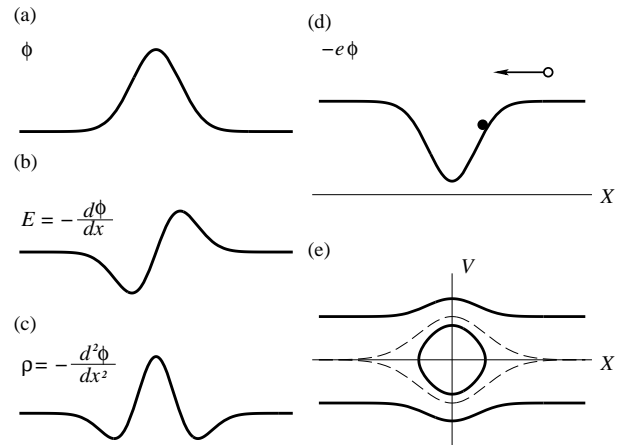


FIG. 1. Please see the text for explanations.

The dashed line marked by electrons with zero total energy is the boundary of the trapping region inside which electrons are trapped and outside which electrons are untrapped. The total energy, $w = \frac{m}{2}v^2 - e\phi$, is a constant of motion. A passing electron ($w > 0$) moves with a constant velocity outside the potential and the speed increases when it encounters the potential pulse and then decreases back to its original value as it moves away. A trapped electron ($w < 0$) bounces back and forth between its two turning points in the potential. Since there is no source or sink for the particles, the density is inversely proportional to the velocity. We can thus deduce that the density of passing electrons is constant outside and becomes smaller as ϕ increases. No excess negative charge results from the passing electrons. On the other hand, trapped electrons have density maxima at their turning points, and so must be responsible for the excess negative charge. The charge density variation (Figure 1(c)) needed to be self-consistent with the solitary potential pulse is thus a net balance of the negative charge from trapped electrons and the positive charge due to the density decrease of passing electrons since the ion density is assumed uniform. From this simple picture, one can see that in BGK solitary waves it is the trapped electrons traveling with the solitary potential that screen out the positive core. Our picture is different from the picture of a positive object in a plasma whose screening is achieved by the thermal motion of the plasma (Debye shielding).

The entire trapping region that consists of the total electron density enhancement at the flanks and depletion at the core is a physical entity produced by the self-consistent interaction between the plasma particles and the solitary potential pulse. This defines the physical identity of one BGK EH. The total charge of the entire trapping region is zero, and therefore it follows that two separated BGK EHs do not interact and the concept of negative mass is not needed.

We now use the approach formulated by BGK [1] to quantify the above arguments and in addition demon-

strate that the results are independent of the strength of the nonlinearity. The time-independent, coupled Vlasov and Poisson equations with the assumption of a uniform neutralizing ion background take the following form:

$$v \frac{\partial f(v, x)}{\partial x} + \frac{1}{2} \frac{\partial \phi}{\partial x} \frac{\partial f(v, x)}{\partial v} = 0, \quad (1)$$

$$\frac{\partial^2 \phi}{\partial x^2} = \int_{-\infty}^{\infty} f(v, x) dv - 1, \quad (2)$$

where f is the electron distribution function and the units have been normalized such that x is normalized by the Debye length, λ_D , energy by the ambient electron thermal energy, T_e , velocity by $v_t = \sqrt{2T_e/m}$, ϕ by T_e/e . The total energy $w = v^2 - \phi$ under this convention. $f = f(w)$ is a solution to Eq. 1 as can be readily verified. Recognizing this, Eq. 2 can be re-written in the following form,

$$\frac{\partial^2 \phi}{\partial x^2} = \int_{-\phi}^0 dw \frac{f_{tr}(w)}{2\sqrt{w+\phi}} + \int_0^{\infty} dw \frac{f_p(w)}{2\sqrt{w+\phi}} - 1, \quad (3)$$

where $f_{tr}(w)$ and $f_p(w)$ are the trapped and passing electron phase space densities at energy w , respectively. The first integral on the RHS of Eq. 3 is the trapped electron density, and the second integral the passing electron density. Prescribe the solitary potential as a Gaussian,

$$\phi(\psi, \delta, x) = \psi \exp(-x^2/2\delta^2), \quad (4)$$

and the passing electron distribution a Maxwellian where the density has been normalized to 1 outside the solitary potential,

$$f_p(w) = \frac{2}{\sqrt{\pi}} \exp(-w). \quad (5)$$

As in BGK approach, we write the trapped electron distribution as

$$f_{tr}(w) = \frac{2}{\pi} \int_0^{-w} \frac{dg(\phi)}{d\phi} \frac{d\phi}{\sqrt{-w-\phi}}, \quad (6)$$

where

$$g(\phi) = \frac{\partial^2 \phi}{\partial x^2} + 1 - \int_0^{\infty} \frac{dw f_p(w)}{2\sqrt{w+\phi}}, \quad (7)$$

is the trapped electron density. The trapped electron distribution obtained through Eq. 6 with the prescribed potential and passing electron distribution yields

$$f_{tr}(\psi, \delta, w) = \frac{4\sqrt{-w}}{\pi\delta^2} \left[1 - 2 \ln \left(\frac{-4w}{\psi} \right) \right] + \frac{2 \exp(-w)}{\sqrt{\pi}} \left[1 - \text{erf}(\sqrt{-w}) \right]. \quad (8)$$

The first term on the RHS of Eq. 8 has been obtained numerically and the second term analytically by Turikov

[8] except for the difference of an overall factor 2 because he defined only half of the phase space density for energy w as $f_{tr}(w)$. Turikov did not explore the details of f_{tr} nor did he calculate the contributions from trapped and passing electrons to macroscopic quantities, such as the charge density, associated with EHs. As shown below, we have relaxed the restriction to empty-centered EHs and taken further steps to unfold the information contained in f_{tr} with emphasis on understanding how a collisionless plasma kinetically supports solitary wave solutions.

The first term in f_{tr} comes from $\partial^2 \phi / \partial x^2$ term in Eq. 7 and has a single peak at $w = \frac{-\psi}{4\epsilon^{3/2}}$. This term is 0 at $w = 0^-$, goes negative at $w = -\psi$, and will always be single peaked even for other bell-shaped solitary potentials (for example, $\text{sech}^2(x/\delta)$ and $\text{sech}^4(x/\delta)$, see Figure 4 of [8] for the special case of empty-centered EHs). Although the peak location may vary, it will not be at the end points, 0 and $-\psi$. The second term arising from the integral of the passing electron distribution monotonically decreases from $w = 0^-$ to $w = -\psi$. The end point behavior of the two terms implies that $f_{tr}(w = 0^-) > f_{tr}(w = -\psi)$. Combining the behavior of the two terms in f_{tr} , it can be concluded that $f_{tr}(0 > w \geq -\psi) \geq f_{tr}(w = -\psi)$. This feature of f_{tr} is essential in making a solitary pulse, and it manifests itself at the peak of the potential as two counterstreaming beams.

f_{tr} is subject to the constraint,

$$f_{tr}(\psi, \delta, w = -\psi) \geq 0, \quad (9)$$

from which we obtain

$$\delta \geq \left[\frac{2\sqrt{\psi}(2 \ln 4 - 1)}{\sqrt{\pi} e^{\psi} [1 - \text{erf}(\sqrt{\psi})]} \right]^{1/2}. \quad (10)$$

Inequality 9 guarantees that $f_{tr}(\psi, \delta, 0 > w \geq -\psi) \geq 0$, since $f_{tr}(0 > w \geq -\psi) \geq f_{tr}(w = -\psi)$ as we have pointed out above. Turikov [8] only considered the special case of empty-centered EHs, which corresponds to the equal sign in inequalities 9 and 10. We plot the width-amplitude relation, Ineq. 10, in Figure 2. A point in the shaded region represents an allowed EH with a given ψ and δ . The shaded region includes all of the allowed ψ and δ for the range of values shown. For a fixed δ , all $\psi \leq \psi_0$ are allowed, where ψ_0 is such that $f_{tr}(\psi_0, \delta, w = -\psi_0) = 0$; while for a fixed ψ , all $\delta \geq \delta_0$ are allowed, where δ_0 is such that $f_{tr}(\psi, \delta_0, w = -\psi) = 0$. This width-amplitude relation is dramatically different from that of KdV solitons whose width-amplitude relation is a one-to-one mapping. There does not exist a minimum size for BGK EHs, and the size need not to be several λ_D [22,9], since one can always adjust ψ so that the RHS of 10 is smaller than the δ that's picked up. We will come back to this issue later in the paper.

With f_p and f_{tr} , we can now calculate the passing and trapped electron densities separately and obtain

$$n_p(\psi, \delta, x) = \int_{-\sqrt{\phi}}^{\infty} f_p(v, x) dv + \int_{-\infty}^{-\sqrt{\phi}} f_p(v, x) dv \\ = \exp(\phi) [1 - \operatorname{erf}(\sqrt{\phi})], \quad (11)$$

$$n_{tr}(\psi, \delta, x) = \int_{-\sqrt{\phi}}^{\sqrt{\phi}} f_{tr}(\psi, \delta, v, x) dv \\ = \frac{-\phi [1 + 2 \ln(\phi/\psi)]}{\delta^2} + \exp(\phi) \operatorname{erf}(\sqrt{\phi}) \\ + \int_{-\sqrt{\phi}}^{\sqrt{\phi}} dv \frac{-\exp(\phi - v^2)}{\sqrt{\pi}} \operatorname{erf}(\sqrt{\phi - v^2}). \quad (12)$$

The integration of the third term in Eq. 12 carried out by a change of variable $y = \sqrt{\phi - v^2}$ and integrating by parts sequentially yields $1 - \exp(\phi)$. Another way to obtain the expression for n_{tr} comes directly from solving Eq. 7 which is essentially the Poisson equation. This yields

$$n_{tr} = \frac{\partial^2 \phi}{\partial x^2} + 1 - n_p \\ = \frac{-\phi [1 + 2 \ln(\phi/\psi)]}{\delta^2} + 1 - \exp(\phi) [1 - \operatorname{erf}(\sqrt{\phi})],$$

which is identical to Eq. 12. Solving Eq. 7 for n_{tr} is simpler, but without the knowledge of f_{tr} , one is not guaranteed whether the particular set of (ψ, δ) is physically allowed ($f_{tr} \geq 0$).

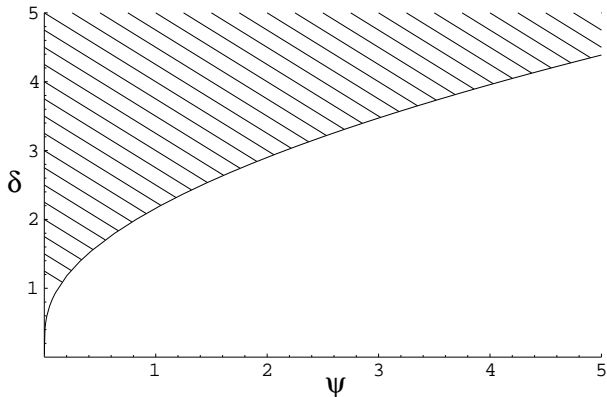


FIG. 2. the width-amplitude relation of BGK EHs that are not restricted to be empty-centered for a Gaussian potential and Maxwellian ambient electron distribution

To study the contributions from trapped and passing electrons to the charge density $(-\partial^2 \phi / \partial x^2)$ and how such contributions are affected by various parameters, we show in Figures 3-5 plots of $n_{tr}(\psi, \delta, x)$ and $n_p(\psi, \delta, x)$ and the charge density ρ as a function of x for several values of ψ and δ . Figure 3 plots $100 \times n_{tr}(2 \times 10^{-5}, 0.1, x)$, $100 \times [n_p(2 \times 10^{-5}, 0.1, x) - 1]$, and $100 \times \rho$. For an ambient plasma with $T_e = 700eV$ and $\lambda_D = 100m$ as found at ionospheric heights by FAST satellite in the environment

of BGK EHs [17], this case corresponds to $\psi = 1.4 \times 10^{-2}V$ and $\delta = 10m$. As shown, in this weakly nonlinear case, the maximum perturbation in n_p is only 0.5% and in n_{tr} 0.4%. The perturbation in the charge density ρ is $\leq 0.2\%$, and occurs all within one λ_D .

We plot $n_p(5, 4.4, x)$ and $n_{tr}(5, 4.4, x)$, and the corresponding ρ in Figure 4. This choice corresponds to a point nearly located on the curve $f_{tr}(w = -\psi) = 0$ in Figure 2 and is an extremely nonlinear case. One can see that the total charge density perturbation goes $\sim 10\%$ negative and $\sim 25\%$ positive, corresponding respectively to electron density enhancement and depletion. With similar format, Figure 5 plots a case with same δ and $\psi = 1$ to illustrate the change in n_p , n_{tr} , and ρ of an EH with equal width but smaller amplitude. By locating this case in Figure 2, one notices that farther away from the $f_{tr}(w = -\psi) = 0$ curve, the dip in n_{tr} is filled up and the charge density perturbation only increases to 5% positive and 2% negative.

These examples demonstrate how trapped electrons produce negative charge density perturbations and passing electrons positive charge density perturbations owing to the decrease in their number density. It is always true that $n_{tr} \geq 0$, since the number density cannot be negative, and therefore trapped electrons always contribute to negative charge density regardless of the strength of the nonlinearity. This result disagrees with the picture that the positive core is due to a deficit of deeply trapped electrons, and that this positive core is screened out by the ambient electrons [9]. It is also different from the conclusion that the trapped electrons are screened out by the resonant or nonresonant passing electrons depending on the EH velocity in [22].

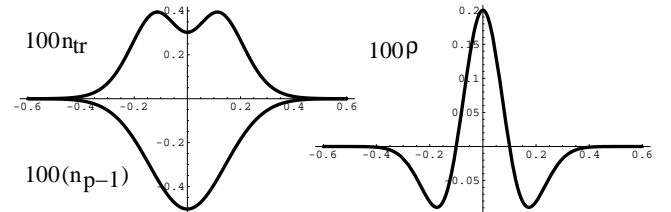


FIG. 3. Trapped electron density (n_{tr}), passing electron density (n_p), and charge density (ρ) for $\psi = 2 \times 10^{-5}$ and $\delta = 0.1$.

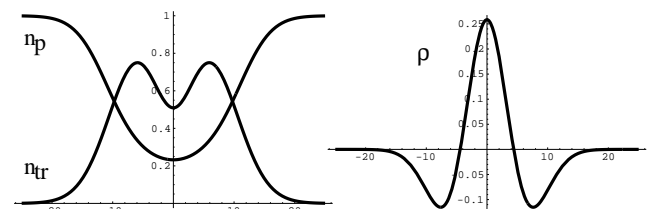


FIG. 4. Trapped electron density (n_{tr}), passing electron density (n_p), and charge density (ρ) for $\psi = 5$ and $\delta = 4.4$.

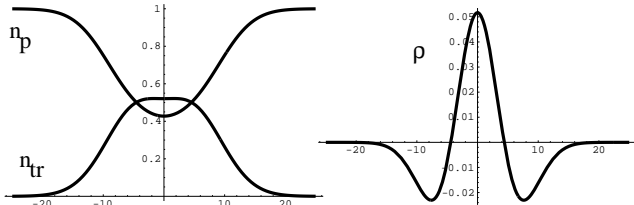


FIG. 5. Trapped electron density (n_{tr}), passing electron density (n_p), and charge density (ρ) for $\psi = 1$ and $\delta = 4.4$.

We now return to the issue of minimum size of EHs. From the illustrations of Figures 3-5, one sees that the trapped electrons have to distribute and oscillate in such a way to result in the desired negative charge at the flanks to shield out the positive core. The entire solitary object is a self-consistent and self-sustained object with zero total charge and does not require thermal screening. Thus, the size of EHs are not restricted to be greater than λ_D .

The charge density variations (ρ) in Figures 4 and 5 suggest that the maximum excursion of ρ is proportional to ψ for fixed δ , as $Max(\rho)$ decreases from 25% to 5% when ψ varies from 5 to 1. This relation can be quantified in the following way:

$$\begin{aligned} Max(\rho) &\equiv \rho(x = 0) \\ &= -n_{tr}(x = 0) - n_p(x = 0) + 1 = \psi/\delta^2, \end{aligned} \quad (13)$$

which shows that when δ is fixed, $\rho(x = 0)$ varies linearly with ψ from 0 to ψ_0/δ^2 , where ψ_0 is such that $f_{tr}(\psi_0, \delta, w = -\psi_0) = 0$ (the curve in Figure 2). Eq. 13 although obtained from a particular case of a Gaussian potential is actually a general relation that holds for bell-shaped potentials. We can examine the generality of Eq. 13 by a dimensional analysis: since the potential amplitude and width are the only two characteristic scales involved in the second spatial derivative of the potential, the maximum excursion of the charge density (that is $-\partial^2\phi/\partial x^2|_{x=0}$) is proportional to ψ/δ^2 . We can also examine how $\rho(x = 0)$ varies along the curve $f_{tr}(w = -\psi) = 0$ (empty-centered EHs) by writing δ as a function of ψ . Eq. 13 then becomes

$$\rho(x = 0)_{ec} = \frac{\sqrt{\pi}\sqrt{\psi}e^\psi[1 - \text{erf}(\sqrt{\psi})]}{2(4\ln 2 - 1)}, \quad (14)$$

where the subscript ec stands for empty centered. The RHS of Eq. 14 tends to zero as $\sqrt{\psi}$ for $\psi \ll 1$, and approaches the constant $1/2(4\ln 2 - 1)$ for $\psi \gg 1$. In other words, for empty-centered EHs the maximum charge density excursion does not increase indefinitely with ψ but settles to a constant value. Since for a physical solution, one would not expect $Max(\rho)$ to increase indefinitely, we can take $Max(\rho)$ approaching a constant at large ψ ($\gg 1$) as a general behavior for bell-shaped solitary potentials. It then implies that for large ψ , the width-amplitude relation $\delta \propto \sqrt{\psi}$ holds in general. For $\psi \ll 1$, we can only deduce that δ must approach zero

in a manner faster than $\sqrt{\psi}$ in order to meet the physical requirement that $Max(\rho)$ goes to zero with ψ . This general width-amplitude relation that we obtained for empty-centered EHs is independent of the specific functional form of the solitary potential and is consistent with what Turikov [8] obtained for two special profiles of potentials, $\text{sech}^2(x/\delta)$ and $\text{sech}^4(x/\delta)$.

In summary, we obtained the trapped electron distribution function for a Gaussian potential and a Maxwellian passing electron distribution following the BGK approach, and showed that the charge density variation is the net balance of the negative charge produced by trapped electrons and the positive charge density produced by a depletion of passing electrons inside the solitary potential. It is not the thermal screening from the ambient electrons that shields out the positive core of the EH, but the oscillations of trapped electrons in between their turning points that result in the excess negative charge. We showed that a BGK EH consists of an electron density enhanced region and depletion region, and this means that the total charge for a BGK EH is zero. It thus follows that two separated EHs do not interact and the concept of negative mass is not needed. It also indicates that there does not exist a minimum size for BGK EHs. These features are independent of the particular choice of potential profile and passing electron distribution, and also independent of the strength of non-linearity. The restriction to empty-centered EHs which was used previously is relaxed to obtain a more general width-amplitude relation that is not a one-to-one mapping but of an inequality form. The maximum charge density excursion is shown to be proportional to ψ and inversely proportional to δ , and approaches a constant for $\psi \gg 1$. It is also argued that for BGK EHs that are empty-centered, the width-amplitude relation for $\psi \gg 1$ takes the common form $\delta \propto \sqrt{\psi}$, and for $\psi \ll 1$, δ approaches zero faster than $\sqrt{\psi}$.

In the above calculation, the EHs do not have relative motion with respect to the ambient electrons. However, this does not restrict us to non-moving EHs, since the entire ambient electron population can have a finite mean velocity $\langle v \rangle_{e-i}$ with respect to the ions (whose frame is taken to be the observer frame) as long as $\langle v \rangle_{e-i}/v_t$ lies within the threshold of Buneman instability [23], where v_t is the ambient electron thermal velocity. In fact, it has been shown that a finite $\langle v \rangle_{e-i}$ is needed for the long term stability of BGK EHs to ensure that ions do not participate in the dynamics of the solitary pulses [24]. The inclusion of a finite EH velocity with respect to the ambient electrons will only introduce an asymmetry in the partition between the two directions of the velocity of passing electrons, and will not alter the above conclusions as long as the BGK solutions remain valid, that is, before any instability sets in.

Our result indicates that there is no long range interaction between BGK EHs. Two EHs interact only when

they are in contact. The only factor that can bring two separated EHs closer to each other is their relative velocity. A system with multiple EHs will not evolve into a state with only one single EH, if the EHs are separated and move with equal velocity or if the faster EH moves in front of the slower ones.

Finally, note that the arguments and results we obtained for BGK electron solitary waves can be analogously applied to BGK ion solitary waves.

One of the authors (Chen) is grateful to Bill Peria for the discussions on the electric field experiment onboard FAST satellite. The research at the University of Washington is supported in part by NASA grants NAG5-3170 and NAG5-26580.

- [23] O. Buneman, *Phys. Rev.*, **115**, 503 (1959)
- [24] Y. Omura, H. Matsumoto, T. Miyake, and H. Kojima, *J. Geophys. Res.*, **101**, 2685 (1996)

- [1] I. B. Bernstein, J. M. Greene, and M. D. Kruskal, *Phys. Rev.*, **108**, 546 (1957)
- [2] K. V. Roberts and H. L. Berk, *Phys. Rev. Lett.*, **19**, 297 (1967)
- [3] K. Saeki and H. Genma, *Phys. Rev. Lett.*, **80**, 1224 (1998)
- [4] V. L. Krasovsky, H. Matsumoto, and Y. Omura, *Nonlinear Processes in Geophys.*, **6**, 205 (1999)
- [5] K. Saeki, P. Michelsen, H. L. Pécseli, and J. J. Rasmussen, *Phys. Rev. Lett.*, **42**, 501 (1979)
- [6] J. P. Lynov, P. Michelsen, H. L. Pécseli, and J. J. Rasmussen, *Phys. Scr.*, **20**, 328 (1979)
- [7] H. Washimi and T. Taniuti, *Phys. Rev. Lett.*, **17**, 996 (1966)
- [8] V. A. Turikov, *Phys. Scr.*, **30**, 73 (1984)
- [9] H. Schamel, *Phys. Rep.*, **140**, pp172-173 (1986)
- [10] J. P. Lynov, P. Michelsen, H. L. Pécseli, J. J. Rasmussen, and S. H. Sørensen, *Phys. Scr.*, **31**, 596 (1985)
- [11] H. L. Berk, C. E. Nielsen, and K. V. Roberts, *Phys. Fluids*, **13**, 980 (1970)
- [12] R. Boström, et al., *Phys. Rev. Lett.*, **61**, 82 (1988)
- [13] H. Matsumoto, et al., *Geophys. Res. Lett.*, **21**, 2915 (1994)
- [14] H. Matsumoto, H. Kojima, Y. Omura, I. Nagano, *Geophys. Monogr.*, **105**, New Perspectives on the Earth's Magnetotail, 259 (1998)
- [15] J. R. Franz and P. M. Kintner, J. S. Pickett, *Geophys. Res. Lett.*, **25**, 1277, (1998)
- [16] R. E. Ergun, et al., *Phys. Rev. Lett.*, **81**, 826 (1998)
- [17] R. E. Ergun, C. W. Carlson, L. Muschietti, I. Roth, and J. P. McFadden, *Nonlinear Processes in Geophys.*, **6**, 187 (1999)
- [18] S. D. Bale, et al., *Geophys. Res. Lett.*, **25**, 2929 (1998)
- [19] C. A. Cattell, et al., *Geophys. Res. Lett.*, **26**, 425 (1999)
- [20] L. Muschietti, R. E. Ergun, I. Roth, and C. W. Carlson, *Geophys. Res. Lett.*, **26**, 1093 (1999)
- [21] A. Mälki, H. Koskinen, R. Boström, and B. Holback, *Phys. Scr.*, **39**, 787 (1989)
- [22] V. L. Krasovsky, H. Matsumoto, and Y. Omura, *J. Geophys. Res.*, **102**, 22131 (1997)